Stability Analysis of Interchange-Stable Plasma Sheet to ExB Shear Flow at Substorm Onset

Jason Derr[1], Richard Wolf[1], Stanislav Sazykin[1], Frank Toffoletto[1], and Jian Yang[2]

[1]Rice University
[2]Southern University of Science and Technology

November 21, 2022

Abstract

The shear flow-interchange instability is proposed as the initiating mechanism behind substorm onset. ULF waves occurring within minutes of substorm onset are observed in the magnetotail at frequencies similar to those of the auroral beads, which are a result of a near-earth magnetospheric instability initiating current disruption in the plasma sheet. Growth rates were statistically determined as a function of wavenumber by Kalmoni et al. (2015) using ASI data from a set of substorm events. The RCM-E provides growth phase-evolved runs of background fields for stability analysis of a magnetospheric wave equation for shear flow-interchange modes derived in Derr et al. (2019), from which growth rates and dispersion relations can be calculated for comparison with the statistically-determined growth rates and frequencies of the beads. In the plasma sheet, interchange and shear flow represent a competition between Kelvin-Helmholtz instability and overall interchange stability. On average, flux-entropy increases with radial distance. As the growth phase proceeds, the middle plasma sheet becomes nearly interchange stable, but flux-entropy decreases sharply at the inner edge. Destabilizing shear is weak in the middle of the sheet but quite strong in the SAPS region, earthward of the inner edge. We examine the conditions under which shear can overwhelm interchange stability to trigger instability. Instability phenomenology will be discussed in detail, including discussion of Doppler-resonance structure and a dimensionless parameter W* for characterizing stability domains. Mapping spatial properties to the ionosphere along field lines allows for comparison of instability wavelengths with those of the auroral beads. All substorms terminate in relaxation, either because higher order nonlinearities ultimately suppress growth or due to external conditions which alter the background fields to suppress nonlinear growth. If higher order amplitude expansion terms contribute negatively at some order, then nonlinear relaxation occurs, and a method for determining field saturation values is established.

Stability Analysis of Interchange-Stable Plasma Sheet to $\vec{E} \times \vec{B}$ Shear Flow at Substorm Onset

JASON DERR(1), RICHARD WOLF(1), FRANK TOFFOLETTO(1), STANISLAV SAZYKIN(1) *, JIAN YANG(2)

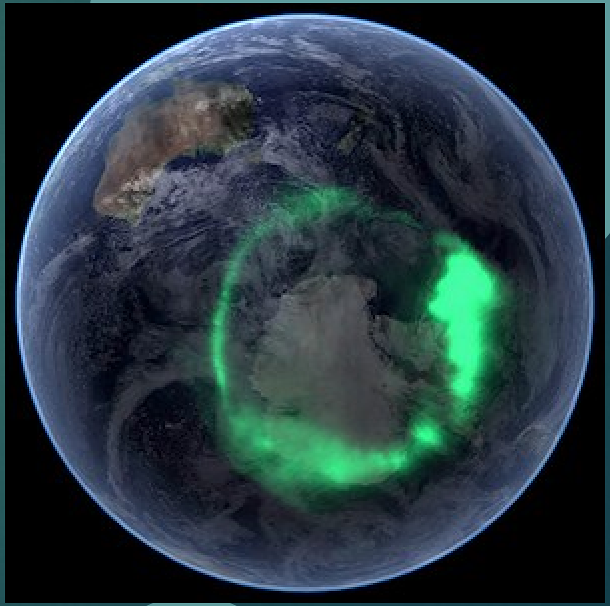

Auroral Beads

- Onset of magnetic substorms pervasively marked by auroral beads.
- Use bead structure to indirectly determine cause of substorm onset.

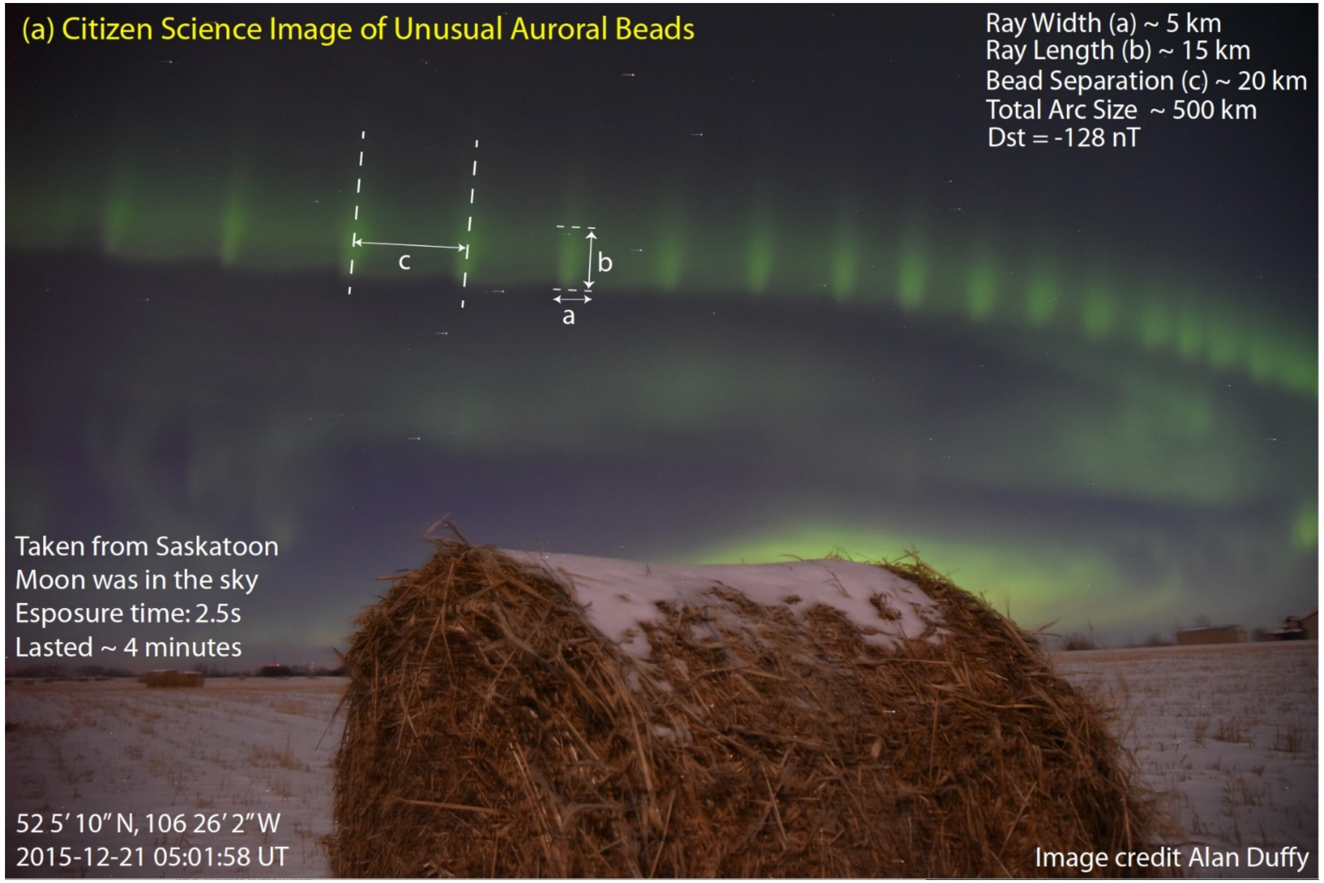

Kalmoni Strategy to Determine Cause of Substorm Onset

- Optical analysis of each substorm from ASI data
- Statistical analysis of many substorms
- Assume beads are the ionospheric projection of a magnetospheric instability
- Compare magnetospheric instability candidates with projected ionospheric signatures

Optical Analysis

- Growth rates as function of wavenumber for determination of most unstable wavenumber (for comparison with theory)
  - Growth rates peak around $\gamma \sim 0.045\ s^{-1}$ at $k_{lon,i} = 2.0 * 10^{-4}\ m^{-1}$
  - Naively mapping to magnetosphere, we obtain $k_{lon,m} = 6.0 * 10^{-6}\ m^{-1}$

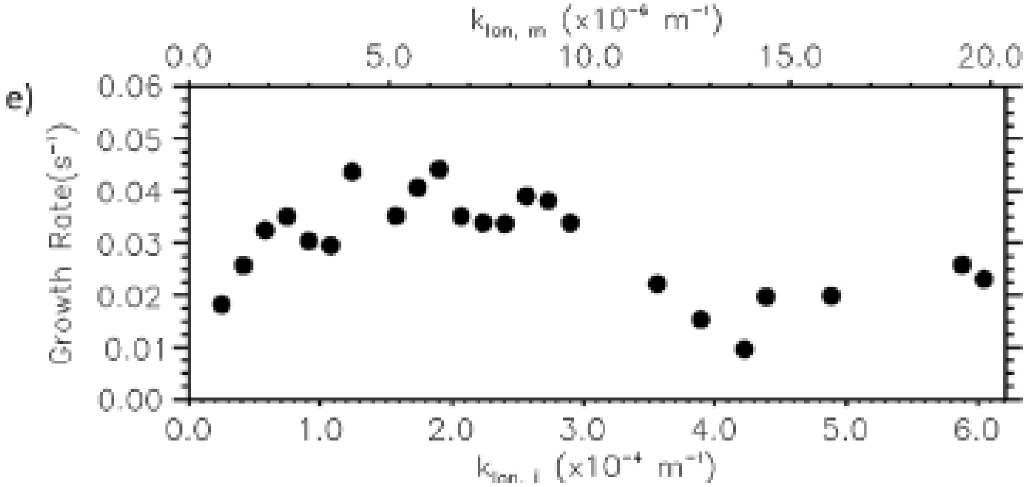

Equilibrium Wedge Model

- Near-Earth nightside of magnetosphere, center of magnetosphere taken to be origin of cylindrical coordinate system (r, φ, y).
- Field lines are concentric circles, and pressure and field strength varies radially. $(P_0, B_0, v_0, K_0, \rho_0)$
- Adiabatic pressure dynamics ($K \coloneqq PV^{\Gamma}$) for flux tubes.
- Flux tube volume $V(r) = r\Delta\varphi / B(r)$.
- No field-aligned conductances
- Equilibrium pressure balance
- System in equilibrium, barring small perturbations which induce no angular motion.

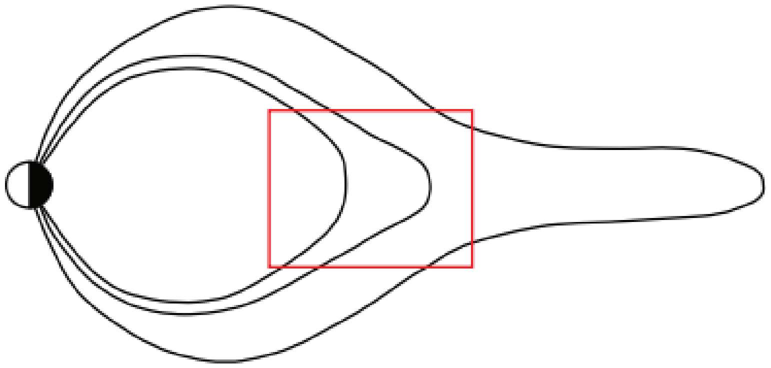

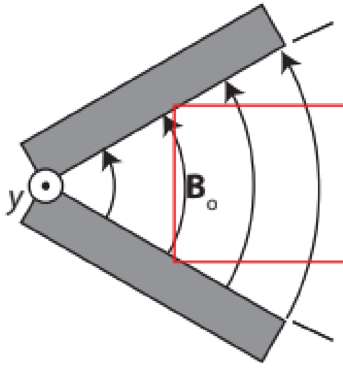

Derivation of Wedge Equation

- Momentum equation and Faraday's (Ohm's) law:
  - $\frac{D}{Dt}(\rho\vec{v}) = -\nabla\left(P + \frac{B^2}{2\mu_0}\right) + \frac{\vec{B}\cdot\nabla\vec{B}}{\mu_0}$
  - $\frac{\partial\vec{B}}{\partial t} = \nabla\times(\vec{v}\times\vec{B})$
- Flux tube adiabaticity serves as closure:
  - $\frac{DK}{Dt} = \frac{D}{Dt}(PV^{\Gamma}) = 0 \rightarrow \frac{D}{Dt}\left(P\left(\frac{r}{B}\right)^{\Gamma}\right) = 0.$
- Definitions:
  - $\widetilde{\omega} \coloneqq \omega - k_y v_0(r)$, $c_A^2 \coloneqq B_0^2/\mu_0\rho_0$, $c_s \coloneqq \Gamma P_0/\rho_0$, $c_f^2 = c_A^2 + c_s^2$.

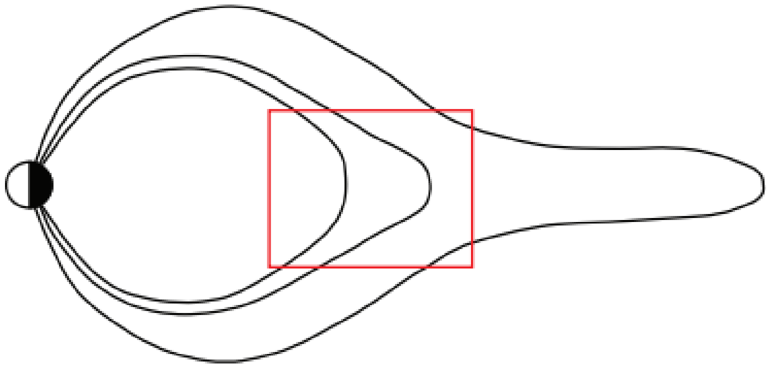

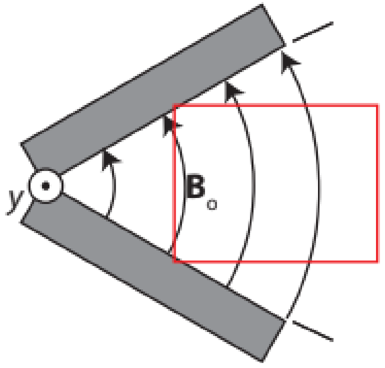

Derivation of Wedge Equation

- Use dawn-to-dusk waves as perturbative normal modes $\delta\blacksquare \sim e^{ik_y y - i\omega t}$.
- Combine to obtain second order decoupled radial velocity equation.
- Take low-frequency limit to obtain equation governing linear stage of shear flow-interchange instability.

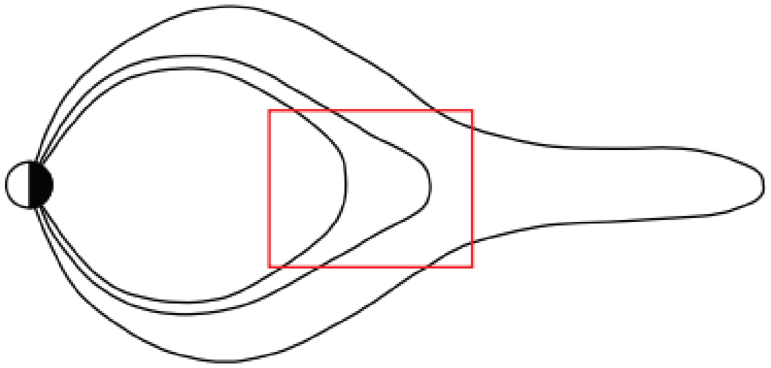

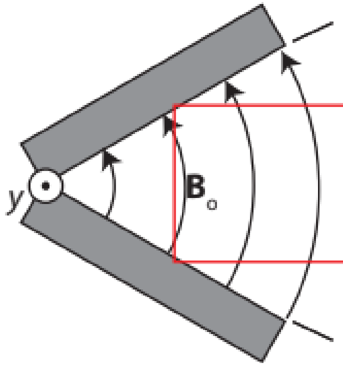

Reduced Low-Frequency Wedge Equation

- Schrödinger Transformation:
  - $\delta u_r'' + V_{eff}(r, \widetilde{\omega}, k_y)\delta u_r = 0$
  - $\delta u_r \coloneqq Ce^{-\frac{1}{2}\int B_{lf}(r)dr}\delta v_r$

$$
\begin{aligned}
V_{eff}(r,\widetilde{\omega},k_y) \;:=\; & \boxed{\frac{k_y v_0''}{\widetilde{\omega}}} - 3\left(\frac{v_0'}{c_f}\right)^2 + \frac{k_y v_0'}{\widetilde{\omega}}\left(\frac{2\widetilde{\omega}^2 - k_y^2 c_s^2 + 3k_y^2 c_A^2}{k_y^2 c_f^2}\right)\frac{\rho_0'}{\rho_0} - \frac{k_y v_0'}{\widetilde{\omega}}\frac{1}{r} \\
& - \frac{3c_s^4 - 10c_s^2 c_A^2 + 3c_A^4}{c_f^4}\frac{1}{4r^2} + \frac{c_s^4 - 2c_s^2 c_A^2 - 3c_A^4}{c_f^4}\frac{1}{2r}\frac{\rho_0'}{\rho_0} - \frac{1}{2}\frac{\rho_0''}{\rho_0} \\
& + \frac{1}{4}\left(\frac{\rho_0'}{\rho_0}\right)^2 - \frac{k_y v_0'}{\widetilde{\omega}}\frac{\widetilde{\omega}^2}{k_y^2 c_f^2}\frac{c_s^2}{c_f^2}\frac{P_0'}{P_0} + \frac{2c_s^2 c_A^2}{c_f^4}\frac{1}{r}\frac{P_0'}{P_0} - \frac{k_y v_0'}{\widetilde{\omega}}\frac{\widetilde{\omega}^2}{k_y^2 c_f^2}\frac{2c_A^2}{c_f^2}\frac{B_0'}{B_0} \\
& - \frac{4c_s^2 c_A^2}{c_f^4}\frac{1}{r}\frac{B_0'}{B_0} + \boxed{\frac{k_y^2 c_f^2}{\widetilde{\omega}^2}\frac{2}{\Gamma r}\frac{c_s^2 c_A^2}{c_f^4}\frac{K_0'}{K_0}} - k_y^2
\end{aligned}
$$

Effective Potential and Fine Array

- First, potential is recast in Laurent series form (with $\omega \coloneqq \omega_r + i\gamma$):
  - $V(r, \omega, k_y) = \frac{1}{\left(v_0(r) - \frac{\omega}{k_y}\right)^2} V_{-2}(r) + \frac{1}{v_0(r) - \frac{\omega}{k_y}} V_{-1}(r) + V_0(r) + V_1(r)\frac{\omega}{k_y} - k_y^2$
- We need a finer array in order to appropriately resolve the resonances. The denominator is:
- $D(r) \coloneqq v_0(r) - \frac{\omega}{k_y} = v_0(r) - \frac{\omega_r + i\gamma}{k_y} \rightarrow v_0' \Delta r - i\frac{\gamma}{k_y}$.

, where the last step results from linearizing velocity near the point $\omega_r = k_y v_0$. So we obtain the following to resolve peaks of interest:

- $\Delta r = \frac{1}{N}\frac{\gamma}{k_y v_0'}, \quad N \gg 1$

Taylor-Goldstein Equation

- The main phenomenological part of our equation, and the part which dominates near the resonances, has the form of a Taylor-Goldstein equation. What I have been calling "pure Kelvin-Helmholtz" is the Rayleigh equation, which is a special case of the Taylor-Goldstein equation with no buoyancy. It can be written in the form:

$$\delta u_r''(r) + \left[W \frac{N^2(z)}{\left(v_0(r) - \frac{\omega}{k}\right)^2} - \frac{v_0''(r)}{v_0(r) - \frac{\omega}{k}} - k^2 \right] \delta u_r(r) = 0$$

where $N(z)$ is the buoyancy frequency.

Richardson's Instability Criterion

- We define the **Richardson's number**:

$$Ri(r) = W = \left(\frac{N(r)}{v_0'(r)}\right)^2$$

- A necessary condition for instability is that $W^* = Ri(r^*) = \min_r Ri(r) < \frac{1}{4}$ somewhere in the domain.

- Basically, in fluid mechanics, our resonances are called "critical layers" and singularities are called "critical points." In intuitive words, "sufficiently strong stratification always has a stabilizing effect."

- Proof of theorem can be found in Kundu's Fluid Mechanics Textbook.

Howards' Semicircle Theorem

- For any unstable eigenvalue ω, real and imaginary components must satisfy:

$$\left(\frac{\omega_r}{k} - \frac{v_{0,max} + v_{0,min}}{2}\right)^2 + \left(\frac{\gamma}{k}\right)^2 \leq \left(\frac{v_{0,max} - v_{0,min}}{2}\right)^2$$

Proof of main theorem can be found in Kundu's Fluid Mechanics Textbook.

- <u>Consequences:</u>

1. Obviously of most importance, this constrains the space of possible eigenvalues.
2. For any marginally unstable mode, there will be singular behavior in the equation.

<u>Proof of 2:</u>

$\frac{\omega_r}{k}$ must be within the range of $v_0(r)$ --> $v_0(r) - \frac{\omega}{k}$ will take on very small values within the radial domain

EXTRA SLIDES

Auroral Beads seen by ASI

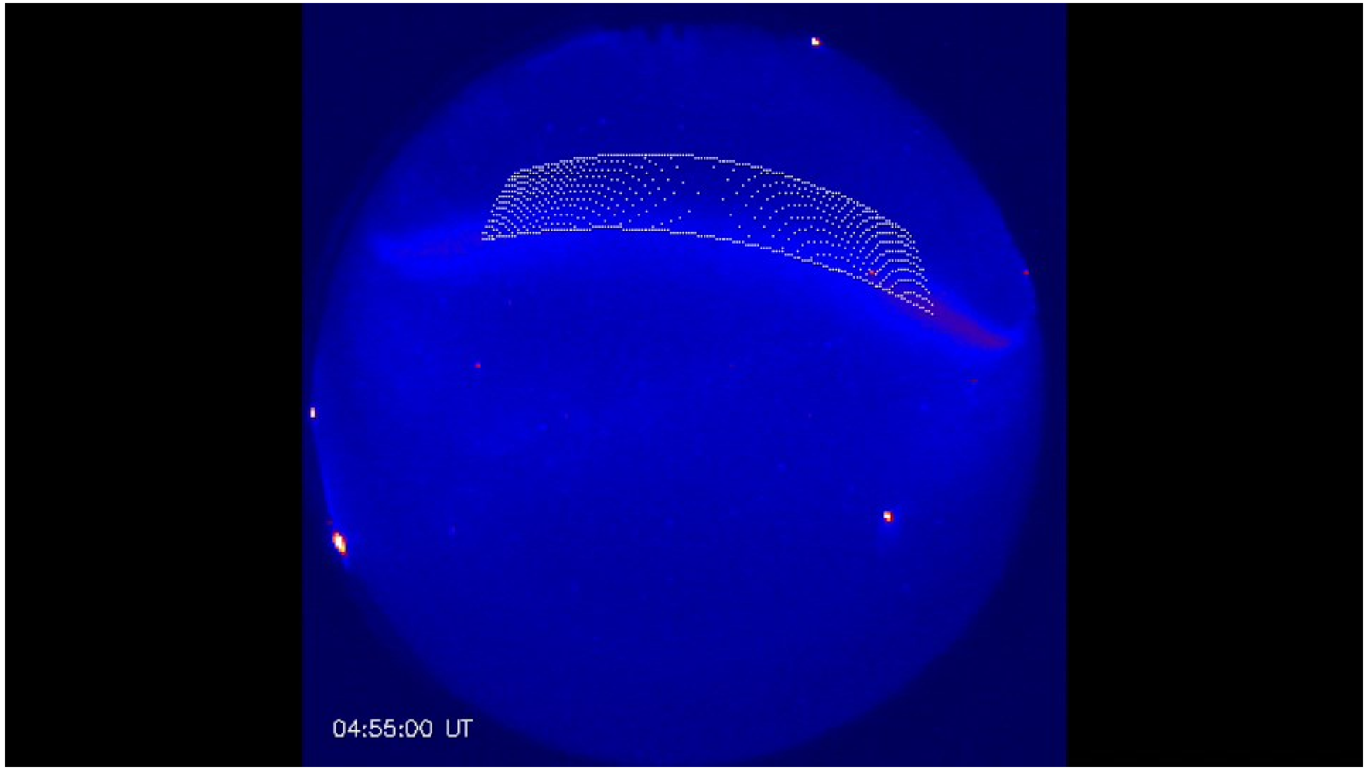

Optical Analysis

- East-west keogram
- Spatial Fourier transform to obtain spatial periodicity information (intensity → PSD)
- Growth rate for each mode (linear growth assumed)

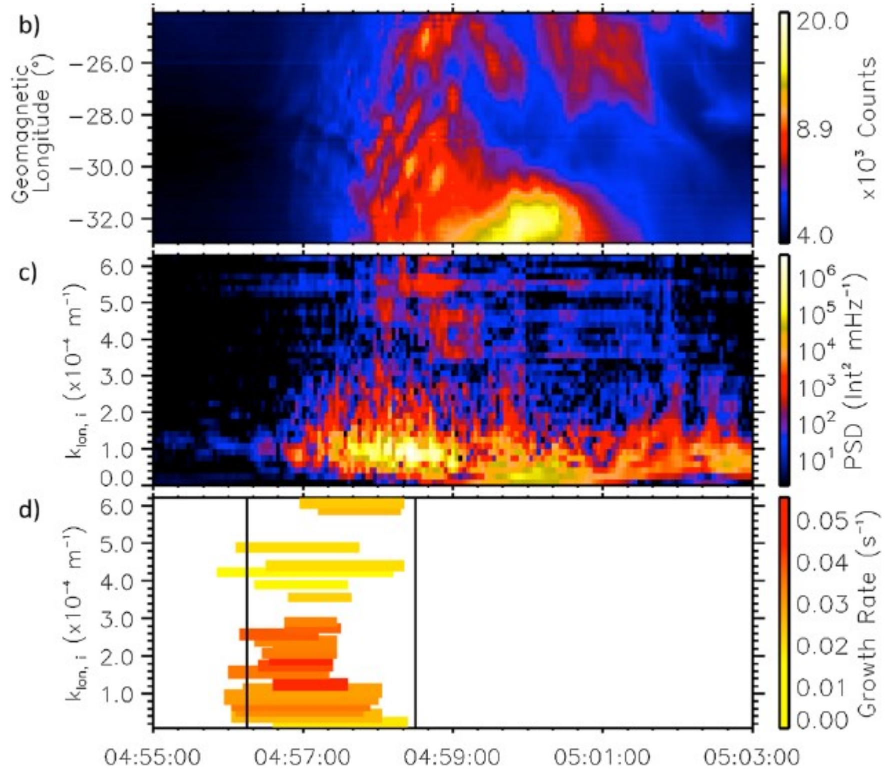

Growth Rate Determination

- Example for exponentially growing mode at $k_{lon} = 0.9 * 10^{-4}\ m^{-1}$

$$\frac{d\delta A(t)}{dt} = \gamma^{*}\delta A(t)$$

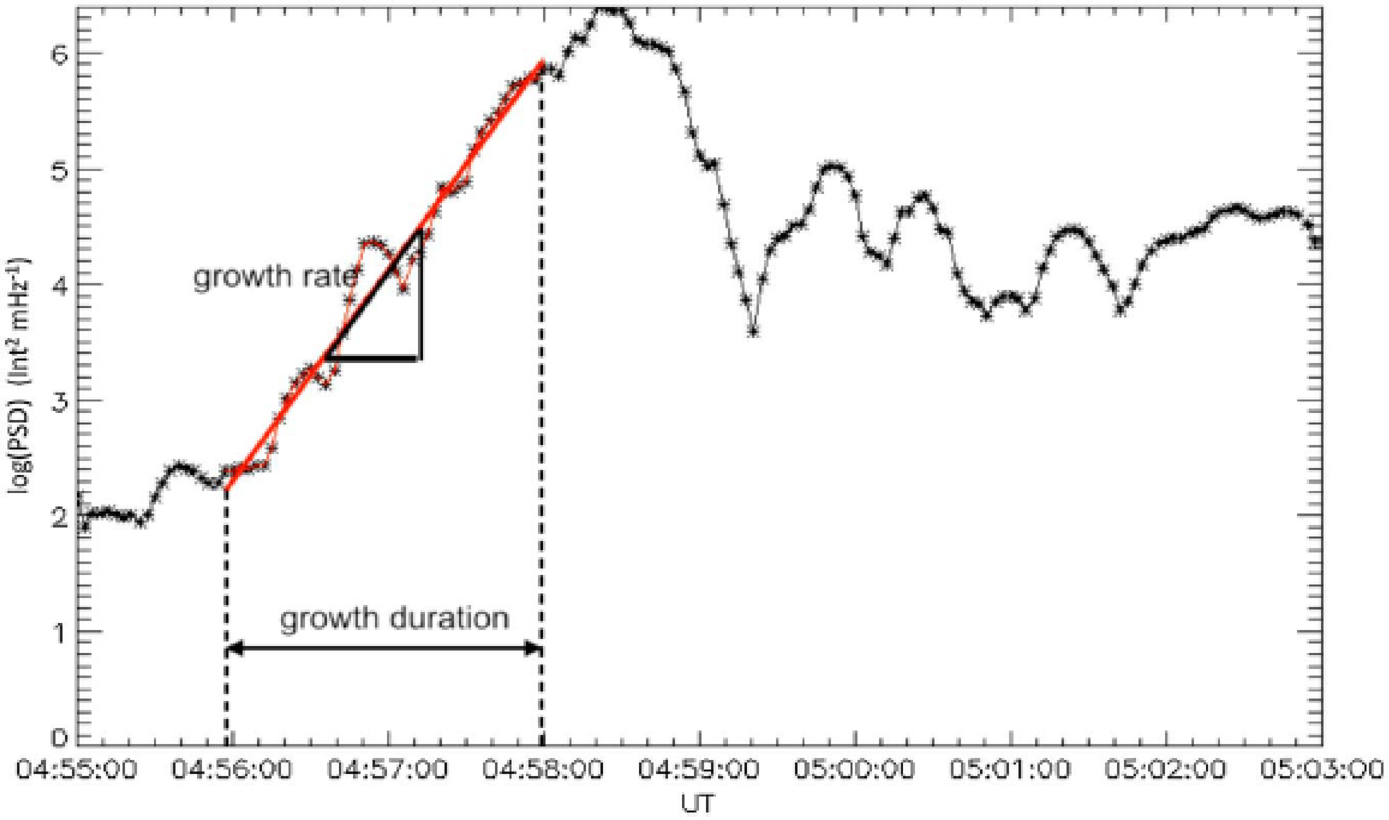

Field-Line Mapping

- Map magnetotail instability along field lines to ionosphere
- Field lines stretch during growth phase
- Kalmoni (2015) used equilibrium model to enact field-line mapping.
  - Underestimates stretching
- We use dynamical model to obtain a better estimate of relevant spatial scales.

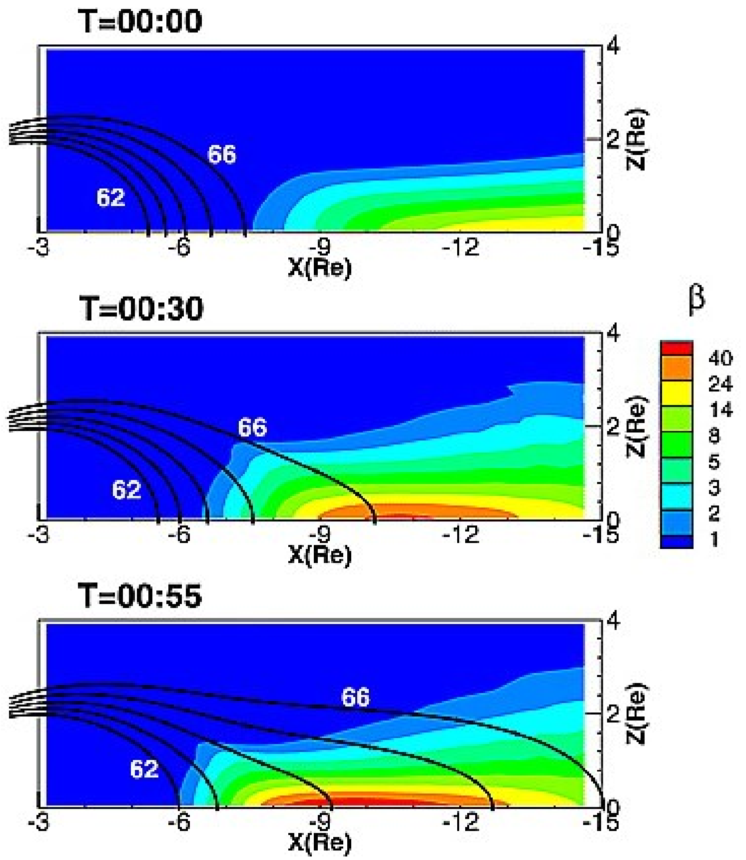

Statistical Analysis of Substorms

- Analysis of 17 substorm events
- Max growth rates range over $[0.03, 0.3]\ s^{-1}$, median $\sim 0.05\ s^{-1}$.
- Ionospheric $k_{lon,i}$ → magnetospheric $k_{lon,m}$ growth rates peak within $k_{lon,m} \in [2.5, 5.0] * 10^{-6}\ m^{-1}$
- Most unstable spatial scales map to $\lambda \approx 1700 - 2500\ km$ in equatorial magnetosphere at $\sim 9 - 12\ R_E$

References

- Derr, J., Horton,W., &Wolf, R. (2019). Shear flow-interchange instability in nightside magnetotail as proposed cause of auroral beads as a signature of substorm onset. J. Geophys. Res. Space Physics.
- Dungey, J.W. (1961). Interplanetary magnetic field and the auroral zones. Physical Review Letters, 6(2), 47-48.
- Kalmoni, N. M. E., Rae, I. J., Watt, C. E. J., Murphy, K. R., Forsyth, C., & Owen, C. J. (2015). Statistical characterization of the growth and spatial scales of the substorm onset arc. J. Geophys. Res. Space Physics, 120, 8503-8516.
- Kepko, L., McPherron, R. L., Amm, O., Apatenkov, S., Baumjohann, W., Birn, J., . . . Sergeev, V. (2015). Substorm current wedge revisited. Space Sci. Rev., 190, 1-46.
- NASA. (2007, January). Themis ground-based all-sky imager (asi) array. https://www.nasa.gov/mission pages/themis/spacecraft/asi.html.
- NASA. (2014, August). The solar wind. https://solarscience.msfc.nasa.gov/SolarWind.shtml.
- Neugebauer, M., Goldstein, B. E., McComas, D. J., Suess, S. T., & Balogh, A. (1995). Ulysses observations of microstreams in the solar wind from coronal holes. J. Geophys. Res., 100, 23389-23395.
- Toffoletto, F., Sazykin, S., Spiro, R., & Wolf, R. (2003). Inner magnetospheric modeling with the rice convection model. Space Sci. Rev., 107, 175-196.
- Wolf, R. A., Tooletto, F. R., Schutza, A. M., & Yang, J. (2018). Buoyancy waves in earth’s magnetosphere: Calculations for a 2-d wedge magnetosphere. J. Geophys. Res. Space Physics, 123.

Temporal Modification Determination

- Use amplitude modulus squared.
- Time-average over oscillations since: $\gamma^* \ll \omega^* \implies \frac{2\pi}{\omega^*} \ll \frac{1}{\gamma^*}$
- Now, we arrive at:

$$\frac{d\,|\delta \bar{A}(t)|^2}{dt} = 2\gamma^* \,|\delta A|^2 + C\,|\delta A|^4$$

- Sign of C determinable for any field from the above and:
  - C > 0 → Nonlinear growth (relaxation at higher order or external suppressor effects).
  - C < 0 → Nonlinear relaxation (see following).

Nonlinear Relaxation

- Solve differential equation:

$$\frac{d\,|\delta\bar{A}(t)|^2}{dt} = 2\gamma^*\,|\delta A|^2 + C\,|\delta A|^4$$

- to obtain:

$$|\delta A(t)|^2 = \frac{2\gamma^*}{C}\frac{1}{\frac{v}{C} * e^{-2\gamma^* t} - 1},$$

- Asymptotically, the field amplitudes saturate at:

$$|\delta A|_{sat} = \sqrt{\frac{2\gamma^*}{C}}$$

Nonlinear Analysis (Spatial Modification)

- Substorm must eventually terminate with relaxation of the auroral beads.
- Linear stage:

$$\frac{\partial}{\partial t} x^i = -i M_1^{ij} x^j$$

$$x_1^j = \begin{bmatrix} \delta P \\ \delta B_\phi \\ \delta v_r \\ \delta v_y \end{bmatrix}$$

- Second order terms included:

$$\frac{\partial}{\partial t} x^i = -i M_1^{ij} x^j + M_2^{ijk} x^j x^k$$

- Truncate and solve for second order vector (spatial modification):

$$x_2^i = -i \left(M_1^{-1} \right)^{ij} M_2^{jkl} x_1^k x_1^l$$

Nonlinear Analysis (Temporal Modification)

- Form of all perturbations including nonlinear modification:

$$\delta A(t)e^{-i\omega_r t}(f(y,r) + \Delta(y,r))$$

- Now, we want to substitute into full matrix equation to determine nonlinear time behavior by obtaining time derivative of $\delta A(t)$. It is only exponential growth at linear stage.

Eliminate Spatial Modifications

$$\frac{\partial}{\partial t}\delta A e^{-i\omega_r t}(f+\Delta) = -iM_1\delta A e^{-i\omega_r t}(f+\Delta) + Q$$

$$e^{-i\omega_r t}(f+\Delta)\frac{\partial}{\partial t}\delta A - i\omega_r \delta A e^{-i\omega_r t}(f+\Delta) = -iM_{1H}\delta A e^{-i\omega_r t}(f+\Delta) - iM_{1AH}\delta A e^{-i\omega_r t}(f+\Delta) + Q$$

$$f\frac{\partial}{\partial t}\delta A + \Delta\frac{\partial}{\partial t}\delta A = -iM_{1AH}\delta A(f+\Delta) + Qe^{i\omega_r t}$$

$$\frac{\partial}{\partial t}\delta A = -if^* M_{1AH}\delta A f + f^* Q e^{i\omega_r t}$$

$$\frac{\partial}{\partial t}\delta A = \gamma\delta A + f^* e^{i\omega_r t} Q$$

- 1. Chain Rule (L), Matrix Split (R)
- 2. Multiply by $e^{i\omega_r t}$, Hermitian cancellation
- 3. Multiply by f^*, Anti-Hermitian cancellation
- 4. Simplify Anti-Hermitian term